Journal of Biomolecular NMR, 10 (1997) 283–288
KLUWER/ESCOM

J-Bio NMR 484

Specific ^{15}N, NH correlations for residues in ^{15}N, ^{13}C and fractionally deuterated proteins that immediately follow methyl-containing amino acids

D.R. Muhandiram[a], Philip E. Johnson[b], Daiwen Yang[a], Ouwen Zhang[a], Lawrence P. McIntosh[b] and Lewis E. Kay[a]

[a]*The Protein Engineering Centers of Excellence and Departments of Medical Genetics, Biochemistry and Chemistry, University of Toronto, Toronto, ON, Canada M5S 1A8*
[b]*The Protein Engineering Centers of Excellence, Department of Chemistry and Department of Biochemistry and Molecular Biology, University of British Columbia, Vancouver, BC, Canada V6T 1Z3*

Received 16 June 1997
Accepted 28 July 1997

Keywords: ^{15}N,^{13}C,^{2}H-labeled proteins; ^{2}H spin relaxation; ^{15}N, NH correlations

Summary

A triple-resonance pulse scheme is described which records ^{15}N, NH correlations of residues that immediately follow a methyl-containing amino acid. The experiment makes use of a ^{15}N, ^{13}C and fractionally deuterated protein sample and selects for CH_2D methyl types. The experiment is thus useful in the early stages of the sequential assignment process as well as for the confirmation of backbone ^{15}N, NH chemical shift assignments at later stages of data analysis. A simple modification of the sequence also allows the measurement of methyl side-chain dynamics. This is particularly useful for studying side-chain dynamic properties in partially unfolded and unfolded proteins where the resolution of aliphatic carbon and proton chemical shifts is limited compared to that of amide nitrogens.

The use of deuteration in concert with triple-resonance spectroscopy has greatly facilitated the assignment of backbone ^{15}N, ^{13}C and NH resonances as well as side-chain ^{13}C chemical shifts (Grzesiek et al., 1993b; Yamazaki et al., 1994; Farmer and Venters, 1995). This is largely the result of the considerable lengthening of the transverse relaxation times of the carbons and remaining protons which occurs upon substitution of deuterons for protons in the molecule of interest (Yamazaki et al., 1994; Venters et al., 1996). A number of different deuteration strategies have recently been proposed, including the preparation of proteins that are (randomly) deuterated at levels ranging from 50% to 100% (Grzesiek et al., 1993b; Yamazaki et al., 1994; Nietlispach et al., 1996) and the production of molecules with high levels of deuteration combined with specific enrichment of protons at sites such as methyl groups of hydrophobic residues (Metzler et al., 1996; Rosen et al., 1996; Smith et al., 1996; Gardner and Kay, 1997). The advantages and disadvantages associated with each of the strategies have been discussed elsewhere (Kay and Gardner, 1997).

One of the first steps in the sequential assignment of proteins is the identification of spin systems which serve as distinctive starting points in the assignment process. This can be accomplished with selective ^{15}N labeling, for example (McIntosh and Dahlquist, 1990). More recently, pulse sequences have been developed which establish correlations for only a subset of the residues in uniformly ^{15}N, ^{13}C-labeled proteins (Grzesiek and Bax, 1993a; Olejniczak and Fesik, 1994; Gehring and Guittet, 1995). Amino acids such as Gly, Thr and Ser are excellent entry points for assignment since the $^{13}C^{\alpha}$ chemical shifts of Gly and the $^{13}C^{\alpha}/^{13}C^{\beta}$ shifts of Thr and Ser are well removed from the corresponding $^{13}C^{\alpha}$ and $^{13}C^{\beta}$ shifts of other residues. Wagner and co-workers have recently developed a suite of experiments which aids in the backbone assignment of ^{15}N, ^{13}C-labeled proteins by correlating ^{15}N, $^{13}C^{\beta}$ and NH shifts of aromatic residues or of Asx exclusively, making use of the fact that the C^{γ} carbons of these residues have distinct chemical shifts (Dötsch et al., 1996a). They have also shown that it is possible to select for Gly, Ala, Ser and Cys on the basis of the fact that these residues do not con-

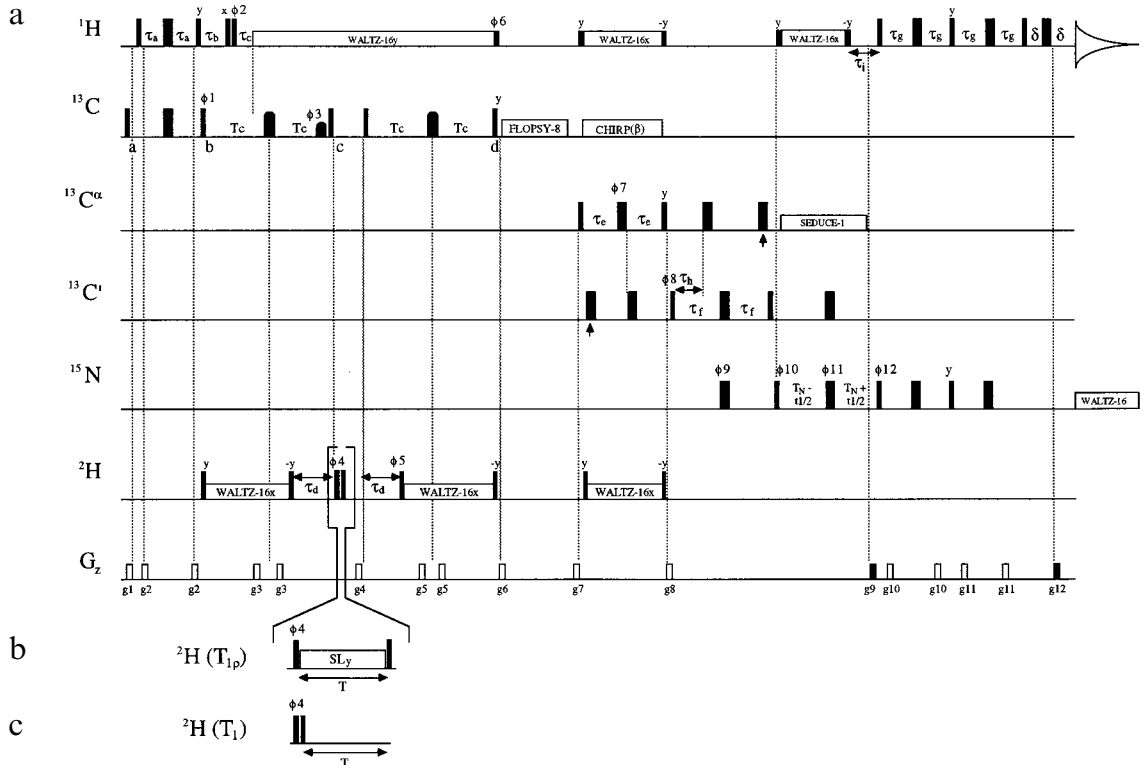

Fig. 1. (a) Pulse scheme used to measure ^{15}N, NH correlations of residues that follow methyl-containing amino acids. Experimental details for two related experiments upon which the present sequence is based are given in Muhandiram et al. (1995) and Gardner et al. (1996). A brief description is provided here for completeness. All narrow (wide) pulses are applied with flip angles of 90° (180°) and are along the x-axis, unless otherwise indicated. Carriers are positioned at 4.73 ppm (^{1}H), 119 ppm (^{15}N), 0.8 ppm (^{2}H), 20 ppm (^{13}C, start of sequence until start of FLOPSY-8 (Mohebbi and Shaka, 1991)), 43 ppm (^{13}C, FLOPSY mixing), or 58 ppm (^{13}C, immediately after FLOPSY-8 until the end of the sequence). Decoupling is interrupted during the application of gradient pulses (Kay, 1993) and, where appropriate, proton and deuterium magnetization from water is restored to the z-axis prior to the gradient pulses (Grzesiek and Bax, 1993b; Kay et al., 1994; Stonehouse et al., 1994). All proton pulses are applied with a 25 kHz field, with the exception of the 6.4 kHz field used both for WALTZ decoupling (Shaka et al., 1983) and for the pulses immediately flanking the decoupling elements. All rectangular ^{13}C pulses between points a and d in the sequence are applied with a 19.5 kHz field. The shaped pulses in the centers of the $2T_c$ periods are 370 μs RE-BURP pulses (Geen and Freeman, 1991) centered at 35 ppm (Boyd and Scoffe, 1989; Patt, 1992) and the $^{13}C^{\alpha}$-selective pulse (600 μs) of phase ϕ3 has the SEDUCE-1 profile (McCoy and Mueller, 1992) with a center of excitation at 57 ppm. TOCSY mixing is achieved using the FLOPSY-8 scheme (8 kHz field, 8 cycles). All $^{13}C^{\alpha}$ pulses are applied to minimize excitation in the ^{13}C' region of the spectrum and employ field strengths of $\Delta/\sqrt{15}$ (90°) and $\Delta/\sqrt{3}$ (180°), where Δ is the separation in Hz between the centers of the $^{13}C^{\alpha}$ and ^{13}C' regions (Kay et al., 1990). In a similar manner, all ^{13}C' pulses are applied with a field strength of $\Delta/\sqrt{15}$. $^{13}C^{\beta}$ decoupling is achieved using WURST pulses (Fu and Bodenhausen, 1995; Kupce and Freeman, 1995), as described in Gardner et al. (1996), while $^{13}C^{\alpha}$ decoupling (during $2T_N$) employs a WALTZ-16 field with 310 μs pulses having the SEDUCE-1 profile. All ^{15}N pulses are applied with a 5.3 kHz field and decoupling during acquisition employs a 1.1 kHz field. ^{2}H decoupling is achieved using a 0.7 kHz field, while 2.1 kHz flip-back pulses flank each decoupling element. Bloch–Siegert compensation pulses are indicated with the vertical arrows (Vuister and Bax, 1992). The delays employed are as follows: $\tau_a = 1.7$ ms, $\tau_b = 3.95$ ms, $\tau_c = 1.98$ ms, $T_c = 14.5$ ms, $\tau_d = 11$ ms, $\tau_e = 3.7$ ms, $\tau_f = 12.4$ ms, $\tau_g = 2.2$ ms, $\tau_h = 4.4$ ms, $\tau_i = 5.5$ ms, $T_N = 12.4$ ms, $\delta = 0.5$ ms. The phase cycling is ϕ1 = 2(x),2(–x); ϕ2 = x,–x; ϕ3 = 4(x),4(–x); ϕ4 = 4(x),4(–x); ϕ5 = 4(–y),4(y); ϕ6 = –x,x; ϕ7 = 8(x),8(–x); ϕ8 = 8(x),8(–x); ϕ9 = 16(x),16(–x); ϕ10 = x; ϕ11 = 2(x),2(–x); ϕ12 = x; rec. = x,2(–x),x,–x,2(x),–x. After 8 scans the phase of the receiver is inverted. The durations and strengths of the gradients are g1 = (0.5 ms, 5 G/cm), g2 = (0.3 ms, 3 G/cm), g3 = (0.3 ms, –25 G/cm), g4 = (0.4 ms, –10 G/cm), g5 = (0.2 ms, 10 G/cm), g6 = (0.6 ms, 15 G/cm), g7 = (1.0 ms, 15 G/cm), g8 = (0.5 ms, 7.5 G/cm), g9 = (1.25 ms, 30 G/cm), g10 = (0.2 ms, 2.5 G/cm), g11 = (0.3 ms, 3 G/cm), g12 = (0.125 ms, 29.6 G/cm). Quadrature detection is achieved in t_1 using the enhanced sensitivity gradient approach, where for each value of t_1 N- and P-type coherences are obtained by recording data sets with the sign of the gradient g9 inverted and 180° added to the phase of ϕ12 (Kay et al., 1992; Schleucher et al., 1993). For each successive increment of t_1, 180° is added to ϕ10 and to the phase of the receiver (Marion et al., 1989). (b) Pulse scheme used to record the decay of C_zD_y, replacing the region in brackets. A 1.0 kHz ^{2}H spin-lock field is employed. (c) Sequence used to record the decay of C_zD_z, replacing the bracketed portion in the main scheme.

tain C^{γ} carbons (Dötsch et al., 1996b) or Thr, Val and Ile since the C^{β} carbons of these amino acids are one-bond-coupled to only a single proton (Dötsch et al., 1996c).

In the present communication we wish to add to the list of experiments which select for particular spin systems by describing a pulse scheme which establishes ^{15}N, NH correlations of residues in ^{15}N, ^{13}C and fractionally deuterated proteins that are immediately C-terminal to amino acids with methyl-containing side chains. The experiment is thus useful both during the initial stages of assignment and for the confirmation of assigned shifts obtained on the basis of existing triple-resonance experiments. In addition, a variation of the experiment is presented which allows the measurement of methyl side-chain dynamics in

cases where ^{13}C and ^{1}H chemical shifts of methyl groups are overlapped yet backbone ^{15}N, NH correlations are resolved. An example is provided in the case of the protein Δ131Δ, a 131-residue fragment of staphylococcal nuclease which is a model system for studying unfolded protein states (Shortle, 1996).

Figure 1a illustrates the pulse scheme from which ^{15}N, NH correlations of residues that immediately follow methyl-containing amino acids are obtained. The initial part of the sequence extending from points a to d in the figure is similar to an experiment for measuring ^{2}H relaxation times of $^{13}CH_2D$ methyl groups in fractionally deuterated, uniformly ^{13}C-labeled proteins that has recently been described (Muhandiram et al., 1995). The second half of the experiment is based on HC(CO)NH-TOCSY pulse schemes and relays magnetization from methyl sites to the C^{α} carbon and subsequently to the NH of the following amino acid via transfer steps involving the intervening $^{13}C'$ (carbonyl) and ^{15}N spins (Logan et al., 1992; Montelione et al., 1992; Grzesiek et al., 1993a). The magnetization transfer pathway can be summarized by

$$\begin{aligned} &^{1}H^{m} \xrightarrow{J_{CH}} {}^{13}C^{m} \xrightarrow{J_{CD}} {}^{13}C^{m}D \xrightarrow{J_{CD}} {}^{13}C^{m} \xrightarrow{J_{CC}} \\ &{}^{13}C^{\alpha} \xrightarrow{J_{C\alpha C'}} {}^{13}C' \xrightarrow{J_{CN}} {}^{15}N(t_1) \xrightarrow{J_{NH}} NH(t_2) \end{aligned} \quad (1)$$

where $^{1}H^{m}$ and $^{13}C^{m}$ correspond to methyl proton and carbon magnetization, respectively, $^{13}C^{m}D$ denotes the magnetization state C_zD_z, where C_z and D_z are the z components of carbon and deuterium magnetization (point c in the sequence), the active couplings responsible for magnetization transfer are indicated above each arrow and t_i is an acquisition time.

A number of filtering schemes have been included in the sequence of Fig. 1 to ensure that only magnetization which originates on methyl groups gives rise to an observable signal at the NH of the subsequent residue. This is achieved by selecting for $^{13}CH_2D$ methyl types. At point b in the sequence, the magnetization of interest is of the form I_zC_{TR} (I_z is the z component of proton magnetization and C_{TR} is transverse carbon magnetization) and during the subsequent delay $\tau_b = 1/(2J_{CH})$ the signal evolves due to the one-bond ^{13}C-^{1}H scalar coupling to give

$$\begin{aligned} &I_zC_{TR} \xrightarrow{\tau_b} C_{TR} && (CHD_2 \text{ methyls, CH methines, CHD methylenes}) \\ &I_z^iC_{TR} \xrightarrow{\tau_b} I_z^jC_{TR}, \quad i \neq j && (CH_2D \text{ methyls, } CH_2 \text{ methylenes}) \\ &I_z^iC_{TR} \xrightarrow{\tau_b} I_z^jI_z^kC_{TR}, \quad i \neq j \neq k && (CH_3 \text{ methyls}) \end{aligned} \quad (2)$$

where the superscripts i,j,k distinguish the individual methyl protons and all multiplicative factors have been omitted. Immediately following the τ_b period, a ^{1}H $90_x90_{\phi 2}$ pulse pair is applied where the phase $\phi 2$ is cycled (+,–) with concomitant inversion of the receiver phase (Muhandiram et al., 1995). This selects for carbon magnetization that is antiphase to an odd number of proton spins, such as is the case for a signal originating from CH_2D methyl groups or CH_2 methylenes. A second filtering step occurs by selecting for magnetization of the form C_zD_z at point c in the pulse scheme with the ^{2}H $90_{\phi 4}90_x$ pulse pair. This selection process eliminates signals which originate from CH_2 methylene groups which would otherwise give rise to ^{15}N, NH correlation peaks.

As described above, the elimination of a signal originating from CHD methylenes is achieved by the τ_b-^{1}H $90_x90_{\phi 2}$ element in the sequence. This scheme also eliminates magnetization from CH methines, CHD_2 and CH_3 methyls, although in the case of CH and CH_3 groups the signal can be completely eliminated by selection for C_zD_z. The efficiency of the ^{1}H filter is based on the uniformity of one-bond J_{CH} couplings for aliphatic proton–carbon pairs so that it is possible to select a unique τ_b value for which Eq. 2 is valid. In practice, this is of course not possible, and subsequently a small number of additional peaks may arise in spectra from magnetization originating on CHD groups. It is straightforward to separate out contributions from CHD and CH_2D moieties by noting that during the τ_b period the signal of interest from CH_2D methyls evolves due to scalar coupling as

$$\begin{aligned} 2I_z^iC_y \xrightarrow{\tau_b} \quad & 2I_z^iC_y \cos^2(\pi J_{CH3}\tau_b) \\ & -2I_z^jC_y \sin^2(\pi J_{CH3}\tau_b) \\ & -0.5C_x \sin(2\pi J_{CH3}\tau_b), \quad i \neq j \end{aligned} \quad (3)$$

while the signal from CHD groups evolves according to

$$2I_zC_y \xrightarrow{\tau_b} 2I_zC_y \cos(\pi J_{CH2}\tau_b) - C_x \sin(\pi J_{CH2}\tau_b) \quad (4)$$

where J_{CH3} and J_{CH2} are the one-bond couplings for methyl and methylene groups, respectively. It is of interest to note that within a given class of carbons, such as methyls or methylenes, the J_{CH} values can vary in an amino acid dependent manner, but this level of complexity is not relevant here (Zwahlen et al., 1997). Choosing $\tau_b = 1/(2J_{CH3})$ selects for the middle term of Eq. 3, but also ensures that the first term of Eq. 4 is retained with an intensity given by $\cos(0.5\pi J_{CH2}/J_{CH3})$. However, if a τ_b value which satisfies the relation $\tau_b < 1/(2J_{CH2,l})$ is chosen, where $J_{CH2,l}$ is the largest J_{CH} value for methylene groups, cross peaks arising from CHD groups are of opposite intensity relative to peaks from methyls and are thus easily distinguished. The similarity of J_{CH2} and J_{CH3} values ensures that a suitable value of τ_b can be found for which very little intensity of the desired peaks is lost. A database of J_{CH} values that we have compiled from a number of proteins establishes that $J_{CH2,l} \sim 147$ Hz (Zwahlen et al., 1997).

Figure 2 illustrates the ^{15}N, NH correlation map of the 152 amino acid N-terminal cellulose-binding domain from *Cellulomonas fimi* 1,4-β-glucanase CenC (CBD_{N1}) (John-

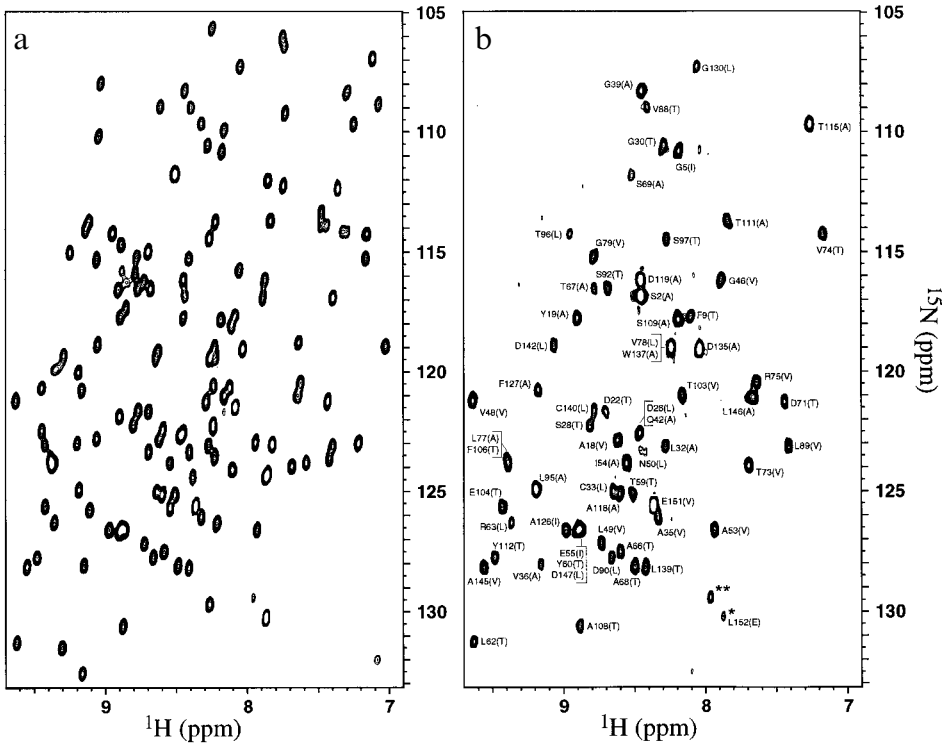

Fig. 2. (a) ^{15}N, NH correlation spectrum (Kay et al., 1992) of a 1.9 mM sample of ^{15}N, ^{13}C, ~50% ^{2}H CBD_{N1}, 50 mM sodium chloride, 50 mM sodium acetate (d_3), 0.02% sodium azide, 4.2 mM calcium chloride, 10% D_2O/90% H_2O, pH 5.9, saturating quantities (3.2 mM) of cellopentaose, 35 °C, recorded on a 600 MHz Varian Inova spectrometer. (b) Spectrum illustrating the ^{15}N, NH correlations of residues that immediately follow methyl-containing amino acids. The residue type from which magnetization originates is indicated in brackets beside each cross peak. The peak labeled * is of opposite phase relative to all the other peaks and arises from magnetization transfer from a CHD group of Glu^{151}. The peak labeled ** is due to an impurity. The spectrum was recorded with acquisition times of 22 and 64 ms in (t_1,t_2) and the time domain signal in t_1 was doubled using mirror image linear prediction (Zhu and Bax, 1990). A relaxation delay of 1.35 s was employed, giving rise to a total acquisition time of 8 h. CBD_{N1} was prepared by overexpression in 40% D_2O/60% H_2O media using 2 g/l (protio) glucose, 1 g/l 50% ^{2}H, 99% ^{13}C, 99% ^{15}N Celtone (Martek) and 1 g/l ^{15}N ammonium chloride. Assignments are from Johnson et al. (1996a,b).

son et al., 1996a,b) in complex with cellopentaose (a) and the corresponding spectrum where only cross peaks of residues that immediately follow a methyl-containing amino acid are obtained (b). The spectra were recorded on a 1.9 mM uniformly ^{15}N, ^{13}C, ~50% fractionally deuterated sample, and in the case of (b) a τ_b delay tuned to a J_{CH} value of 126.5 Hz was employed. Three of the 69 methyl-containing residues precede prolines and therefore do not give rise to ^{15}N, NH correlation peaks in the figure. All of the expected peaks are observed in the spectrum, although correlations for Asn^{50} (Leu^{49}→Asn^{50}), Ser^{69} (Ala^{68}→Ser^{69}) and Thr^{96} (Leu^{95}→Thr^{96}) are weak. In a similar spectrum recorded on CBD_{N1} in the absence of sugar, 64 of the expected 66 correlations were observed, with cross peaks to Phe^{127} (Ala^{126}→Phe^{127}) and Gly^{130} (Leu^{129}→Gly^{130}) missing. Finally, it is noteworthy that for the τ_b value used in the present case (see above) the only peak observed from magnetization associated with CHD groups arises from the penultimate residue, Glu^{151} (Glu^{151}→Leu^{152}). This cross peak (labeled L152 in the figure) is of opposite phase relative to all of the other correlations (CH_2D) in the spectrum. Glu^{151} is highly flexible, giving a very strong ^{15}N, NH cross peak in HSQC spectra of CBD_{N1}. No other anomalous correlations are observed in this spectrum. However, when the delay τ_b is tuned for a J_{CH} value of 140 Hz, two additional cross peaks arising from Glu^{104} (Glu^{104}→Thr^{105}) and Glu^{149} (Glu^{149}→Val^{150}) are observed with the same phase properties as the peak from Glu^{151}.

Our original interest in developing the present pulse scheme was to measure methyl side-chain dynamics in unfolded and partially unfolded proteins, where aliphatic ^{13}C and ^{1}H resolution is limiting (Shortle, 1996). In contrast, the ^{15}N chemical shift dispersion in such molecules is far better and can be exploited to obtain information about more poorly resolved sites. In this regard, we have recently developed a suite of experiments for measuring NOEs involving aliphatic sites in partially unfolded protein states which record backbone ^{15}N and ^{13}C' chemical shifts (Zhang et al., 1997a). Figures 1b and c illustrate the schemes employed to measure ^{2}H $T_{1\rho}$ and T_1 values of $^{13}CH_2D$ methyls in cases where resolution in aliphatic ^{13}C and ^{1}H dimensions is poor. A series of ^{15}N, NH correlation maps are obtained as a function of the delay T, with the intensity profile of each cross peak relating directly to the dynamics of the CH_2D methyl group(s) attached to

the preceding amino acid. For amino acids with two methyl groups (Val, Leu and Ile), only a qualitative interpretation of the data is possible, since the decay of ^{15}N, NH correlation peaks reflects the dynamics at both methyl sites. Note that immediately prior to the period labeled T in (b) and (c), the magnetization of interest is of the form C_zD_y or C_zD_z and it is the decay of these terms that is measured in the $T_{1\rho}$- or T_1-based experiments. The Hamiltonian, H, which gives rise to the relaxation of either C_zD_y or C_zD_z during the delay T can, to excellent approximation, be written as

$$\mathcal{H} = \mathcal{H}^Q(D) + \mathcal{H}^D(CD) + \mathcal{H}^D(I^jC) + \mathcal{H}^D(I^kC) + \mathcal{H}^D(C^lC) + \mathcal{H}^D(I^jD) + \mathcal{H}^D(I^kD),\ k\neq j \quad (5)$$

where $\mathcal{H}^Q(D)$ is the quadrupolar Hamiltonian for spin D and $\mathcal{H}^D(AB)$ is the dipolar Hamiltonian describing the relaxation of spin B from the dipolar coupling with spin A. In Eq. 5, D, C, I^j and I^k are the $^{13}CH_2D$ methyl deuterium (D), carbon (C) and proton (I^j,I^k) spins, while C^l is the carbon spin one-bond-coupled to C. Note that we have included only autocorrelation terms; a previous study has established that cross-correlation effects are negligible (Yang and Kay, 1996). The relative contributions of each of the terms listed in Eq. 5 to the relaxation of C_zD_y or C_zD_z have been calculated previously (Muhandiram et al., 1995), and for completeness will be summarized here for the case of C_zD_z:

$$\begin{aligned}
&\mathcal{H}^Q(D): && 3/16\,(e^2qQ/\hbar)^2\,[J(\omega_D) + 4J(2\omega_D)]\\
&\mathcal{H}^D(CD): && \gamma_C^2\gamma_D^2\hbar^2/(4r_{CD}^6)\,[3J(\omega_D) + 12J(\omega_C) + 6J(\omega_C+\omega_D) + J(\omega_C-\omega_D)]\\
&\mathcal{H}^D(I^{j,k}D): && \gamma_I^2\gamma_D^2\hbar^2/(4r_{ID}^6)\,[J(\omega_I-\omega_D) + 3J(\omega_D) + 6J(\omega_I+\omega_D)] \qquad (6a)\\
&\mathcal{H}^D(I^{j,k}C): && \gamma_I^2\gamma_C^2\hbar^2/(4r_{IC}^6)\,[J(\omega_I-\omega_C) + 3J(\omega_C) + 6J(\omega_I+\omega_C)]\\
&\mathcal{H}^D(C^lC): && \gamma_C^4\hbar^2/(4r_{CC}^6)\,[J(0) + 3J(\omega_C) + 6J(2\omega_C)]
\end{aligned}$$

where

$$J(\omega) = (2/5)S^2\tau_m/[1+(\omega\tau_m)^2] + (1-S^2)\tau/[1+(\omega\tau)^2] \quad (6b)$$

In Eq. 6b τ_m is the overall correlation time for the assumed isotropic rotation, $\tau^{-1} = \tau_m^{-1} + \tau_e^{-1}$, where τ_e is the effective correlation time describing internal motions, and the order parameter, S, is given by $S = S_{axis}[(3\cos^2\theta-1)/2]$, with θ the angle between the dipolar vector in question and the methyl threefold averaging axis. For example, θ is 109.5°, 90° and 0° in the expressions for relaxation originating from the Hamiltonians $\mathcal{H}^Q(D)$, $\mathcal{H}^D(I^{j,k}D)$ and $\mathcal{H}^D(C^lC)$, respectively. The contribution from the quadrupolar interaction to the rate of decay of C_zD_z is given by the first term in Eq. 6a, while the net rate of decay of C_zD_z is derived from the sum of the terms in Eq. 6a. (Note that terms arising from both $\mathcal{H}^D(I^jC)$ and $\mathcal{H}^D(I^kC)$ and from both $\mathcal{H}^D(I^jD)$ and $\mathcal{H}^D(I^kD)$ must be included in the sum; see Eq. 5.)

Numerical evaluation of the terms in Eq. 6 using the following dynamics parameters, $S^2_{axis} = 0.7$, $\tau_e = 25$ ps and 3 ns $\le \tau_m \le$ 30 ns, establishes that the contributions to the relaxation rate of C_zD_z from the various terms in $\mathcal{H}$ are in the order $\mathcal{H}^Q(D) \gg \mathcal{H}^D(I^{j,k}C) > \mathcal{H}^D(CD) \sim \mathcal{H}^D(I^{j,k}D) \sim \mathcal{H}^D(C^lC)$. For example, for $\tau_m = 5$ ns the relative magnitudes of the contributions from $\mathcal{H}^Q(D):\mathcal{H}^D(I^{j,k}C):\mathcal{H}^D(CD):\mathcal{H}^D(I^{j,k}D):\mathcal{H}^D(C^lC)$ are 1.0:0.07:0.003:0.003:0.005. Therefore, to an excellent first approximation the relaxation rate of the double order term, C_zD_z, is given by the first term of Eq. 6a.

As a point of interest, it is worthwhile to consider the difference between the relaxation rates of C_zD_z and C_z $[1/T_1(C_zD_z) - 1/T_1(C_z)]$. In the case of a $^{13}CH_2D$ group, the relaxation of C_z derives from a Hamiltonian of the form

$$\mathcal{H} = \mathcal{H}^D(I^jC) + \mathcal{H}^D(I^kC) + \mathcal{H}^D(C^lC) + \mathcal{H}^D(DC) \quad (7)$$

where the first three terms are as defined in Eq. 6a and $\mathcal{H}^D(DC)$ arises from the dipolar contribution to the relaxation of spin C from spin D. This latter term introduces an additional rate given by

$$\mathcal{H}^D(DC):\ 2\gamma_C^2\gamma_D^2\hbar^2/(3r_{CD}^6)\,[3J(\omega_C)+6J(\omega_C+\omega_D)+J(\omega_C-\omega_D)] \quad (8)$$

Note that the expressions describing the contributions that $\mathcal{H}^D(DC)$ and $\mathcal{H}^D(CD)$ make to the relaxation of C_z (Eq. 8) and C_zD_z (Eq. 6a), respectively, are not identical. Numerical evaluation of the terms in Eqs. 6 and 8, assuming the same range of dynamical parameters as indicated above, establishes that the difference between $[1/T_1(C_zD_z) - 1/T_1(C_z)]$, as measured in a $^{13}CH_2D$ methyl group, and the contribution to the decay of C_zD_z from the quadrupolar interaction, $1/T_1(D)$, is much less than 1% of $1/T_1(D)$. Thus,

$$1/T_1(D) = 1/T_1(C_zD_z) - 1/T_1(C_z) \quad (9a)$$

where $1/T_1(D)$ is given by the first term in Eq. 6a. A similar derivation in the case of an operator of the form C_zD_y indicates that the relation

$$1/T_{1\rho}(D) = 1/T_{1\rho}(C_zD_y) - 1/T_1(C_z) \quad (9b)$$

is equally valid.

In the case of an application to the study of side-chain dynamics of Δ131Δ, we have determined experimentally that $10\times1/T_1(C_z) < 1/T_1(C_zD_z) < 1/T_{1\rho}(C_zD_y)$ and, therefore, the decays of C_zD_y and C_zD_z provide a reasonable measure of the ^2H transverse and longitudinal relaxation rates, respectively. It must be noted that because of the large number of transfer steps in the scheme of Fig. 1 it is difficult to obtain accurate ^2H relaxation times in reasonable measuring periods unless samples are concentrated. Figure 3 illustrates decay curves of C_zD_z and C_zD_y for residues Val^{51}, Val^{66} and Val^{74} from Δ131Δ (4 mM). The $^{13}C^\gamma$ chemical shifts of these residues range from 20.76 to 20.88 ppm (Zhang et al., 1997b), illustrating the resolution problem associated with the study of unfolded and/or partially unfolded protein states.

In summary, we have described a pulse scheme which records ^{15}N, NH correlations of residues immediately fol-

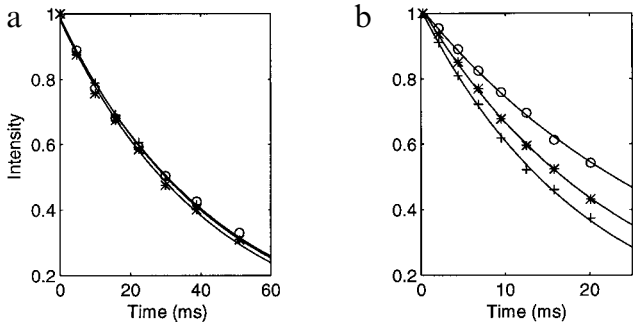

Fig. 3. Decay of C_zD_z (a) and C_zD_y (b) for residues Val^{51} (○), Val^{66} (∗) and Val^{74} (+) of Δ131Δ (4 mM, 1 mM sodium azide, pH 5.3, 32 °C). Each data set from which cross-peak intensities were extracted was recorded in 4 h. T_1 decay times (ms) are 45.0±1.0 (Val^{51}), 42.5±1.0 (Val^{66}) and 44.1±0.7 (Val^{74}), while T_2 values (ms) are 32.3±0.5 (Val^{51}), 23.6±0.3 (Val^{66}), 19.8±0.3 (Val^{74}). Decay values have been obtained assuming equivalent dynamics at both methyl sites.

lowing a methyl-containing amino acid. The experiment is easily modified to measure methyl dynamics using intensity decays of ^{15}N, NH correlation peaks. This is of great utility for the analysis of dynamic properties in unfolded and partially unfolded protein states where the resolution of aliphatic ^1H and ^{13}C chemical shifts is poor. Because the experiment selects CH_2D methyl groups, sensitivity is highest when the level of deuterium incorporation is 33% and the fraction of CH_2D methyl types is 0.44. However, the sensitivity decreases by only 15% when the level of deuterium incorporation is 50%, so that the same sample can be used both for the present experiment, for the assignment of backbone chemical shifts and for NOE-based studies.

Acknowledgements

This work was supported through grants from the Medical Research Council of Canada (L.E.K.) and the Protein Engineering Network Centers of Excellence (L.E.K. and L.P.M.). L.E.K. thanks Dr. David Shortle of Johns Hopkins University for the generous gift of the Δ131Δ sample. L.E.K. is grateful to Dr. Gerhard Wagner (Harvard) for stimulating discussions relating to the relaxation of C_zD_z and C_zD_y terms.

References

Boyd, J. and Scoffe, N. (1989) *J. Magn. Reson.*, **85**, 406–413.
Dötsch, V., Matsuo, H. and Wagner, G. (1996a) *J. Magn. Reson.*, **B112**, 95–100.
Dötsch, V., Oswald, R.E. and Wagner, G. (1996b) *J. Magn. Reson.*, **B110**, 107–111.
Dötsch, V., Oswald, R.E. and Wagner, G. (1996c) *J. Magn. Reson.*, **B110**, 304–308.
Farmer, B.T. and Venters, R. (1995) *J. Am. Chem. Soc.*, **117**, 4187–4188.
Fu, R. and Bodenhausen, G. (1995) *Chem. Phys. Lett.*, **245**, 415–420.
Gardner, K.H., Konrat, R., Rosen, M.K. and Kay, L.E. (1996) *J. Biomol. NMR*, **8**, 351–356.
Gardner, K.H. and Kay, L.E. (1997) *J. Am. Chem. Soc.*, **119**, 7599–7600.
Geen, H. and Freeman, R. (1991) *J. Magn. Reson.*, **93**, 93–141.
Gehring, K. and Guittet, E. (1995) *J. Magn. Reson.*, **B109**, 206–208.
Grzesiek, S., Anglister, J. and Bax, A. (1993a) *J. Magn. Reson.*, **B101**, 114–119.
Grzesiek, S., Anglister, J., Ren, H. and Bax, A. (1993b) *J. Am. Chem. Soc.*, **115**, 4369–4370.
Grzesiek, S. and Bax, A. (1993a) *J. Biomol. NMR*, **3**, 185–204.
Grzesiek, S. and Bax, A. (1993b) *J. Am. Chem. Soc.*, **115**, 12593–12594.
Johnson, P.E., Joshi, M.D., Tomme, P., Kilburn, D.G. and McIntosh, L.P. (1996a) *Biochemistry*, **35**, 14381–14394.
Johnson, P.E., Tomme, P., Joshi, M.D. and McIntosh, L.P. (1996b) *Biochemistry*, **35**, 13895–13906.
Kay, L.E., Ikura, M., Tschudin, R. and Bax, A. (1990) *J. Magn. Reson.*, **89**, 496–514.
Kay, L.E., Keifer, P. and Saarinen, T. (1992) *J. Am. Chem. Soc.*, **114**, 10663–10665.
Kay, L.E. (1993) *J. Am. Chem. Soc.*, **115**, 2055–2056.
Kay, L.E., Xu, G.Y. and Yamazaki, T. (1994) *J. Magn. Reson.*, **A109**, 129–133.
Kay, L.E. and Gardner, K.H. (1997) *Curr. Opin. Struct. Biol.*, in press.
Kupce, E. and Freeman, R. (1995) *J. Magn. Reson.*, **A115**, 273–276.
Logan, T.M., Olejniczak, E.T., Xu, R. and Fesik, S.W. (1992) *FEBS Lett.*, **314**, 413–418.
Marion, D., Ikura, M., Tschudin, R. and Bax, A. (1989) *J. Magn. Reson.*, **85**, 393–399.
McCoy, M. and Mueller, L. (1992) *J. Am. Chem. Soc.*, **114**, 2108–2110.
McIntosh, L.P. and Dahlquist, F.W. (1990) *Q. Rev. Biophys.*, **23**, 1–38.
Metzler, W.J., Wittekind, M., Goldfarb, V., Mueller, L. and Farmer, B.T. (1996) *J. Am. Chem. Soc.*, **118**, 6800–6801.
Mohebbi, A. and Shaka, A.J. (1991) *J. Chem. Phys.*, **178**, 374–377.
Montelione, G.T., Lyons, B.A., Emerson, S.D. and Tashiro, M. (1992) *J. Am. Chem. Soc.*, **114**, 10974–10975.
Muhandiram, D.R., Yamazaki, T., Sykes, B.D. and Kay, L.E. (1995) *J. Am. Chem. Soc.*, **117**, 11536–11544.
Nietlispach, D., Clowes, R.T., Broadhurst, R.W., Ito, Y., Keeler, J., Kelly, M., Ashurst, J., Oschkinat, H., Domaille, P.J. and Laue, E.D. (1996) *J. Am. Chem. Soc.*, **118**, 407–415.
Olejniczak, E.T. and Fesik, S.W. (1994) *J. Am. Chem. Soc.*, **116**, 2215–2216.
Patt, S.L. (1992) *J. Magn. Reson.*, **96**, 94–102.
Rosen, M.K., Gardner, K.H., Willis, R.C., Parris, W.E., Pawson, T. and Kay, L.E. (1996) *J. Mol. Biol.*, **263**, 627–636.
Schleucher, J., Sattler, M. and Griesinger, C. (1993) *Angew. Chem., Int. Ed. Engl.*, **32**, 1489–1491.
Shaka, A.J., Keeler, T., Fenkiel, T. and Freeman, R. (1983) *J. Magn. Reson.*, **52**, 335–338.
Shortle, D. (1996) *Curr. Opin. Struct. Biol.*, **6**, 24–30.
Smith, B.O., Ito, Y., Raine, A., Teichmann, S., Ben-Tovim, L., Nietlispach, D., Broadhurst, R.W., Terada, T., Kelly, M., Oschkinat, K., Shibata, T., Yokoyama, S. and Laue, E.D. (1996) *J. Biomol. NMR*, **8**, 360–368.
Stonehouse, J., Shaw, G.L., Keeler, J. and Laue, E.D. (1994) *J. Magn. Reson.*, **B107**, 178–184.
Venters, R.A., Farmer, B.T., Fierke, C.A. and Spicer, L.D. (1996) *J. Mol. Biol.*, **264**, 1101–1116.
Vuister, G.W. and Bax, A. (1992) *J. Magn. Reson.*, **98**, 428–435.
Yamazaki, T., Lee, W., Arrowsmith, C.H., Muhandiram, D.R. and Kay, L.E. (1994) *J. Am. Chem. Soc.*, **116**, 11655–11666.
Yang, D. and Kay, L.E. (1996) *J. Magn. Reson.*, **B110**, 213–218.
Zhang, O., Forman-Kay, J.D., Shortle, D. and Kay, L.E. (1997a) *J. Biomol. NMR*, **9**, 181–200.
Zhang, O., Kay, L.E., Shortle, D. and Forman-Kay, J.D. (1997b) *J. Mol. Biol.*, in press.
Zhu, G. and Bax, A. (1990) *J. Magn. Reson.*, **90**, 405–410.
Zwahlen, C., Legault, P., Vincent, S.J.F., Greenblatt, J., Konrat, R. and Kay, L.E. (1997) *J. Am. Chem. Soc.*, **119**, 6711–6721.